Research Article
Volume 16:2, 2025

Hydrology: Current Research

ISSN: 2157-7587 Open Access

Integrated Hydrological and Hydraulic Models for Investigation of Channel Morphological Change and River Bank Erosion: A Case of Mersa River, Ethiopia

Yonatan Tibebu[1*], Hussen Ali[2], Fikru Fentan[2] and Yohannes Wodaje[3]

[1]*Department of Water Resources and Irrigation Engineering, Woldia University, Woldia, Ethiopia*

[2]*Department of Water Resources and Irrigation Engineering, Wollo University, Kombolcha Institute of Technology, Kombolcha, Ethiopia*

[3]*Department of Water Resources and Irrigation Engineering, Kombolcha Agricultural College, Kombolcha, Ethiopia*

Abstract

The land use/cover change and other natural and human factors in catchments result in changes in discharge and sediment supply. As a result, the river morphology becomes altered. Morphological change of natural rivers in terms of vertical adjustment and horizontal planform is an important indicator of true channel stability and has a significant effect on lateral bank retreats. The overall goal of this research is to look up the morphological change in rivers and the effect that occurred within the Mersa river. Two commonly used models: the HEC-RAS and SWAT models were used in combination. The first, model SWAT was used to analyze the hydrologic responses of the watershed. Subsequently, the SWAT model's outputs (streamflow and sediment) were then used as input into the hydraulic model HEC-RAS, for simulation of the hydraulics of the river along 2.1 km of the Mersa river to investigate the vertical adjustment, bank erosion, and stability. The river center lines, banks, and width of the river were digitized from acquired satellite images from the years 2010, 2015, and 2020. Different planform metrics such as Sinuosity, Braidedness index, width-to-depth ratio, grain size distribution, and roughness were calculated to investigate the planform changes. The result showed that the change in Sinuosity values for the years 2010, 2015, and 2020 were 1.117, 1.107, and 1.214 respectively. Also, the Braidedness index value estimated as 1.162 (2010), 1.247 (2015), and 1.469 (2020), and the width to depth ratio are above 40 m/m. Additionally, the studied reach of Mersa river was characterized by both aggrading and degrading natures alternatingly with an average aggrading and degrading value of 0.062 m/y and 0.081 m/y respectively. Morphological changes in the river reach included a combination of river bank erosion, vertical bed change, and channel widening, which leads to damaged properties, and any hydraulic structure. Therefore, appropriate conservation measures should be implemented to control the failure of river banks and river vertical bed changes and to prevent the study reach from further land loss and other damage.

Keywords: River morphology • Mersa river • Vertical bed change • Bank erosion • SWAT • HEC-RAS

Introduction

The change that happened in the morphology of rivers due to complex scouring and deposition processes in the river bed and river bank erosion are the main characteristics of natural rivers. This may result from changes in river sediment transport and flow conditions, due to different stages in the hydrological cycle [1]. The river's morphological change. The river morphological changes can be in the form of size, shape, composition of bed material, slope, and planform, this is due to the variance of channel discharge and volume of sediment entering to river and sediment leaving the river and dynamically by nature. Climate change and rainfall amount can be cause for discharge fluctuation while the cause of sediment change mainly depends on the compositions of the river bed and bank materials. In the watershed, different human activities including sand mining, channelization, and water resource development activities significantly change the river system [2]. As a result, the river reacts to these changes by rapid geomorphic adjustment due to lateral bank erosions and changes in the shape and dimension of the channel [3].

Hence, the detection and identification of river changes should be the primary focus of this research, with helpful recommendations for reducing morphological change, bank erosion, and river shifting. To

***Address for Correspondence:** Yonatan Tibebu, Department of Water Resources and Irrigation Engineering, Woldia University, Woldia, Ethiopia, Tel: 251921002010; E-mail: yonatantibebu77@gmail.com;*

Received: 16 January, 2024, Manuscript No. HYCR-24-125129**; Editor assigned:** 19 January, 2024, PreQC No. HYCR-24-125129 (PQ); **Reviewed:** 05 February, 2024, QC No. HYCR-24-125129; **Revised:** 17 April, 2025, Manuscript No. HYCR-24-125129 (R); **Published:** 24 April, 2025, DOI: 10.37421/2157-7587.2025.16.567

understand the rate and amount of change within a river system, the planform and channel characteristics can be employed as time series data. The different plan form metrics used for morphologic change detection are based on aerial photographs acquired over a range of temporal and spatial scales [4].

In this study, the hydrologic model SWAT and hydraulic model HEC-RAS are integrated to provide a bridge between the nonlinear interactions of the uplands and the river responses at the channel scale. Thus, SWAT models have been used for simulating streamflow and sediment by identifying the effects of land cover/use change, climate change, and mitigation strategies on average annual runoff, evapotranspiration, streamflow, groundwater, and other hydrologic responses. But can be inadequate for investigating in-channel conditions due to their inability to represent channel geometry and channel process with sufficient spatial frequency, so one-dimensional (1-D) hydraulic models like the widely-used hydraulic HEC-RAS are needed for their capacity in simulating channel hydraulics by using sediment and streamflow data from SWAT outputs.

The study watershed Mersa is flat and surrounded by mountains, on the other hand, the slope of the river is also highly steep, and any amount of flood causes the destruction of Mersa town. Totally, the morphological change of Mersa river produces different problems for the people because of sediment deposition and floods over the area by losing the farmer's agricultural land, properties, and any hydraulic structure such as bridge, so these must be solved by assessing the river channel morphological change and river bank dynamics to providing appropriate mitigation measure. The research aims are to assess the bed change (aggradation or degradation) in the river and identify the spot where the highest retreations occurred on the riverbank, to detect the planform changes that occurred in the rivers, and to find the impact of river bank erosion as well as morphological change of the Mersa river on the surrounding environment. This study also helped to acquire the finest comprehension of the causes of river bank failure and subsequently design appropriate preventative measures. Hence, the simulation and future prediction of river morphology are very important for the safe management of waterways and the sustainable development of water resources.

Materials and Methods

Description of the study area

The study was conducted on the Mersa River, which is found in the Awash sub-basin. Mersa watershed is located between 561502.8374N and 577442.57587N UTM, and 1287305.453424E and 1295601.553224E UTM. The total area of the watershed is 53.54 km^2. Mersa river originates from the mountains and drains to the downstream passes in Mersa town. The Mersa town is found in North Wollo, Amhara region, Ethiopia at 495 km from Addis Ababa. Mersa is situated along with country (Ethiopian) highway 2 and the highway passes in the Mersa river (Figure 1).

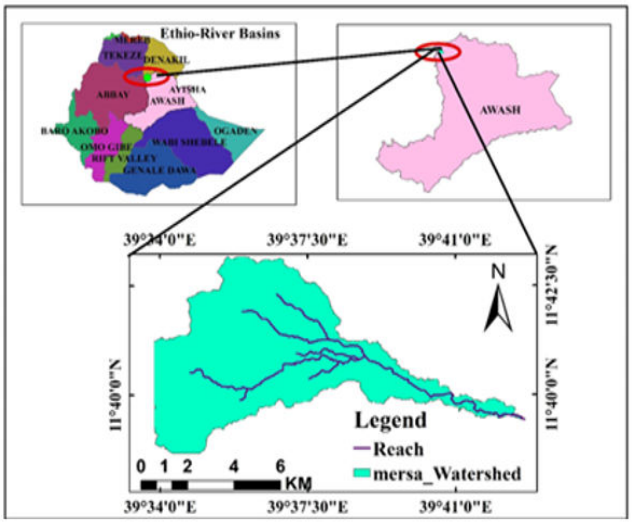

Figure 1. Location map of Mersa watershed.

The elevation of the Mersa watershed ranges from 1473 to 3585 m m.a.s.l between the headwater and downstream. The lower elevation of Mersa is found in the eastern part of the watershed and their higher elevation is found in the western part of the watershed. The mean elevation of the watershed is 2529 m. A large part of the catchment is found below the mean elevation as the elevation map of the watershed is indicated in Figure 2.

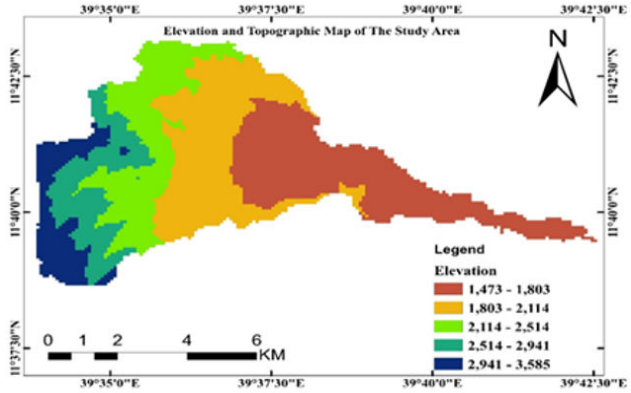

Figure 2. Elevation map of Mersa watershed.

Types of data and their source

Metrological data: The necessary metrological data for this research were rainfall, maximum and minimum temperature, relative humidity, wind speed, and solar radiation which are obtained from sunshine daytime hour data. The meteorological data were used as input for hydrological model (SWAT) development in the watershed. There are some metrological stations used in this research that have 21 and more than 21 years of record metrological values in the watershed. The selection of the representative metrological stations depends on the length of the recording period, availability of climatic variables, the distance from the catchment, and the stations inside and surrounding the Mersa watershed are Woldia, Srinka, Mersa, Wurgesa, Wuchale, and Haike. Twenty-one years of daily rainfall data

(1993-2013) for all stations were obtained from the National Meteorological Agency of Ethiopia (NMAE) (Table 1).

Stations name	Latitude (degree)	Longitude (degree)	Altitude (m.a.s.l)	Rainfall (mm)	Temperature		Time-step (Year)
					Max	Min	
Woldia	11.83	39.59	1897	X	-	-	1993-2013
Sirinka	11.75	39.62	1861	X	X	X	1993-2013
Mersa	11.68	39.66	1578	X	X	X	1993-2013
Wurgesa	11.55	39.62	2000	X	-	-	1993-2013
Wuchale	11.52	39.61	1948	X	-	-	1993-2013
Haike	11.31	39.68	1985	X	X	X	1993-2013

Table 1. Metrological station and availability of data in the Mersa watershed.

Spatial data: The land use land cover, digital elevation model, and soil are the three main spatial data inputs by the hydrological model. A Digital Elevation Model (DEM) is a representation of the topographic surface of the bare ground. and elevation as a digital file of the Earth at any point in a specific resolution, excluding buildings, trees, and any other surface objects. It is used for catchment extraction, hydrologic analysis, and terrain attributes like elevation at any point, slope, drainage basin, and channel network within the watershed (digital elevation model).

The land use land cover spatial datasets describe the types and densities of land use land cover found within a given area. As a result, the land use land cover and soil data were also collected from the Ministry of Water, irrigation, and Energy (MoWIE). The inputs of the hydrological model concern the chemical and physical properties of soil; shapefile formats of soil distribution were collected from the Ethiopian MoWIE GIS department. The water content, soil texture, bulk density, and hydraulic conductivity were extracted from the shapefile of the soil.

Hydrological data: The stream discharge or flow is an important water cycle variable since it combines all the processes occurring in a watershed and provides an output variable that can readily be determined besides serving as an indicator for climate change and variability by reflecting changes in rainfall and evapotranspiration [5]. The study area is a gauged station at Mersa. The streamflow data for the Mersa river was collected from the Ethiopian Ministry of Water, Irrigation, and Electricity for a period of 17 years (1997-2013). However, there is some missing data totally or partially, and short gauge records in streamflow data. Therefore, the missing value was filled. This streamflow was used for performing sensitivity analysis, calibration, and validation of model simulation using the SWAT hydrological model and HEC-RAS hydraulic model.

The annual discharge total of 80-90% occurs in the July to September rainy season. The distribution of the monthly average discharge of Mersa River at the outlet is illustrated below in Figure 3.

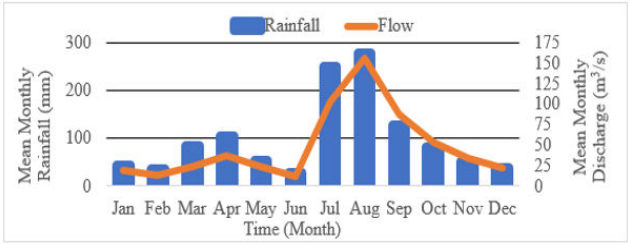

Figure 3. Mean monthly rainfall-runoff distribution in mersa watershed.

Identification of the study reach and demarcation of cross-sectional data: The study reaches were classified into two reaches (upper and lower reaches along the main Mersa river). Changes in the morphology of the river were observed in these two reaches from north to south. The lengths of the whole reach understudy were fixed to 2.1 km based on the sensitivity of the reach for change (1.2 km below the bridge or for lower reach and 0.9 km above the bridge or upper reach).

The river cross-sectional data is a necessary input in the HEC-RAS model and is laid out normal to the direction of flow at a specified measured interval (30 m to 100 m) along the centerline of the main channel. In this study, 47 fixed cross-sections were surveyed and prepared. The downstream reach length is calculated from the difference between two successive coordinates y, or the distance of the points (Figure 4).

Figure 4. A photo shows surveying the river cross-section.

Other hydraulic input data

Roughness coefficients: The method of analytical procedures was used to estimate roughness value by considering the existing channel physical characteristics such as surface roughness, vegetation, channel

plan forms, and bank and bed materials. Due to a slight variation of channel characteristics within the study reach, a uniform n value is taken as an average for all the cross-sections in a reach. That is an average Manning's n for the main channel and an average n for the right and left over banks are taken for all the cross-sections in a reach.

Therefore, the n value for each of the segments is estimated as per the following equation [6].

$n=(n_0+n_1+n_2+n_3+n_4)\ m_5$

Where: n_0=a basic value for a straight, uniform, smooth channel in a natural material involved

n_1=a value-added to no to account for the effect of surface irregularities

n_2=a value for variations in shape and size of the channel x-section

n_3=a value for obstruction

n_4=a value for vegetation and flow condition

m_5=correction factor for meandering of a channel.

The basic value, no, is estimated by the following empirical relations [7]: Developed from channel bank and bed soil material that is done at sieve analysis

$n_0=0.039 \times d_{50}^{1/6}$ (d in feet) Grade and Raju

$n_0=0.047 \times d_{50}^{1/6}$ (d in meter) Subramanya

$n_0=0.038 \times d_{90}^{1/6)}$ (d, meter) Meyer-Peter and Muller

Where di is a grain size in which i percentage of the particles finer than d.

Coefficients of contraction and expansion: By evaluating the gradual or abrupt change (change in channel cross-section variations), and the plan forms, values for expansion and contraction coefficients are estimated for each cross-section. The values of Contraction and expansion coefficients for different channel conditions are given in Table 2.

Channel condition	Coefficient	
	Expansion	Contraction
Gradual change	0.3	0-0.1
Abrupt change	0.5	0.5

Table 2. Contraction and expansion for various channel conditions.

River bed and bank material type, size, and distribution: The proportion of silt, clay, sand, and gravel in the stratigraphy identifies and determines the grain size distribution of both river beds and banks, by the sieve analysis method in the laboratory. The soil samples for river bank material in this study are taken at the same location where the bed material samples are taken.

To get a representative sample of the whole bank, a soil sample was taken at the top, middle, and bottom of the bank and the sample was mixed to get a real representative sample of the bank (Figure 5). Similarly, the soil samples are taken for the bed of the river within the specified reach of the study area (from upper and lower beds) by considering the longitudinal and traversal particle distributions as well as the vertical distribution of the sediment distributions (Figure 6).

According to [8] coarse-grained soils (size>4.75 mm) and a sand fraction (75 μ<size<4.75 mm), the soil retained above sieve diameters of 4.75 mm is considered as gravel. The soil retained between sieve diameters of 0.106 mm to 4.75 mm is considered sand lastly the soil retained at a sieve diameter of 0.075 mm and the pan has taken as fine soil.

Figure 5. The samples of soil material were taken at the bank of the upper reach (A) and taken at the bank of the lower reach (B).

Figure 6. The samples of soil material were taken at the bed of the lower reach (A) and taken at the bed of the upper reach (B).

Data quality analysis of hydro-metrological data

For hydrological modeling and frequency analysis, data quality analysis is important to make sure data that should be complete with no missing values, consistent, homogeneous, and free from trends [9]. The quality of data for this research was analyzed or checked for different conditions like accuracy (check for missing data, outliers, etc.), data adequacy (the length of records), data consistency (using double mass curve), homogeneity test (using a relative method or non-dimensional plot) and check for the absence of a trend and trend analysis (using Spearman's correlation and Mann-Kendall non-parametric trend test).

After analysis of the hydro-metrological data for different conditions like accuracy, adequacy consistency, and general arrangement of the historical flow data, the annual mean discharge, annual maximum

discharge as well as the bank full discharge for a certain return period can be estimated. In addition, the fitted apparent distribution function for the site was selected to estimate flood for the different return periods. There are different methods to select the apparent distribution functions. Out of these methods, the flood frequency analysis method was selected based on the criterion of the availability of historical flood records at the site to forecast extreme flood events [10]. The L-moment parameter estimator method was used to select the appropriate apparent fitted distribution functions by comparing the skewness and kurtosis ratio of the Site estimated with the different frequency distribution functions. Then the best probable parameter distribution for our 17 years of streamflow data is the GEV method. As a result, the 2 return period floods are estimated by the Generalized Extreme Value (GEV) distribution adopted as effective discharge because 1.5 to 2 years return period discharge can be adopted as an effective discharge for perennial rivers.

General methods of the study

To achieve the objectives of this study, the application of two models in an integrated fashion is proposed: a SWAT model and then the HEC-RAS model. This approach, as shown in Figure 7 was proposed to consider large-scale (watershed characteristics) effects on small scales (river characteristics). Maintaining a continuous spatial connection between the models allows the simulation of water fluxes from the watershed to the channel scale for investigating river morphologic effects. Used SWAT for the first component of the modeling cascade (labeled "Hydrologic Model–Watershed Scale"). This model is used for simulating the effects of watershed characteristics, climate, and LULC changes on water fluxes and water balances within the study watershed. However, the watershed SWAT models can be inadequate for investigating in-channel conditions due to their inability to represent channel geometry and channel process with sufficient spatial frequency. Thus the second component of the modeling cascade (labeled "Hydraulic Model–Channel Scale) like the widely-used HEC-RAS is needed for its capacity to simulate channel hydraulics.

The SWAT outputs (Streamflow and sediment) were preprocessed and then used as steady-flow data input for the HEC-RAS model.

In addition, land-sat images digitized and georeferenced by Arc-GIS were used for this study to identify morphological changes (used for Planform change detection) in the recent past, from 2010 to 2020 within 5 years' interval, by different planform metrics such as Braided ness index, Sinuosity, and width-to-depth ratio.

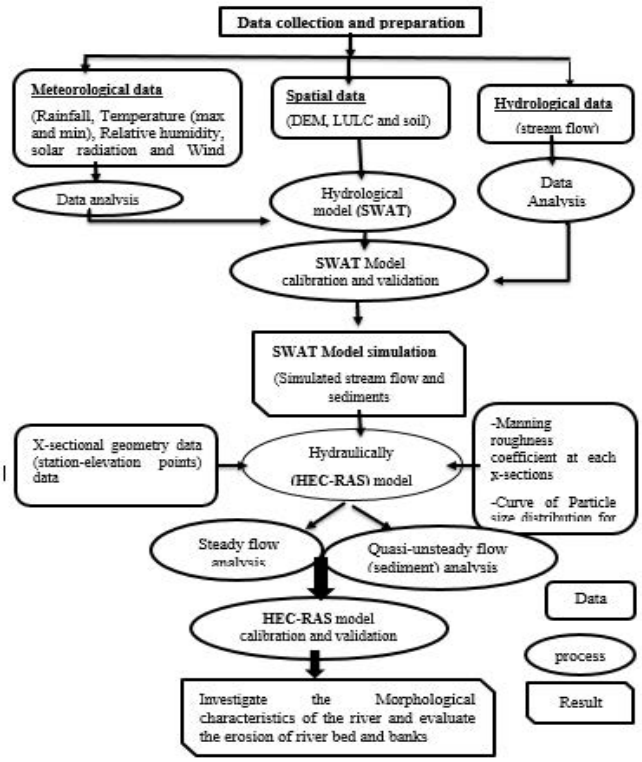

Figure 7. Schematic of the model framework used for this study.

Materials used and their function to conduct the research

To accomplish this research work various materials, programming, and software were used Table 3 below:

ArcGIS 10.4	Used to enter, store, retrieve process, and display spatial information in the form of maps or image geo-referencing, digitization purposes, and other various spatial analysis
ArcSWAT2012	SWAT model development, run execution, present results using reports and maps
XLSTAT 2014	For data quality testing (Homogeneity test and trend analysis) of meteorological and flow data
SWAT_CUP2019	Used for model calibration and validation
UTM Converter	used to convert the coordinates of the stations and gauge stations from geographic to UTM and UTM to geographic
EndNote	To write references within an appropriate format
Landsat imageries	Used for extracting information about the different planform change detection
Total stations	To collect cross-section points in the study reach for geometry input for HEC-RAS
HEC-RAS model	Used to predict erosion deposition patterns of the river bed and predict
Google Earth Pro.	Helps to cross-check the recorded coordinates of the metrological and gauge stations, cross-check the land-use features

Table 3. Tools and software used for this study.

Acquisition and analysis of successive land-sat images and planform change detection

In this study the satellite data between 2010 and 2020, within a 5 years' gap was taken based on a minimum time-period requirement of 5 to 10 years' period for morphological change study of a river reach under consideration the three Land-Sat (ETM+) images with a 30 m spatial resolution were downloaded from the USGS Earth Explorer website. The first images for the year 2010 were Landsat-7 image types whereas the next two images for the years 2015 and 2020 were Landsat-8 images, those land-sat images are digitized each year as a feature class (line) and stored in a geo-database. Arc GIS has digitized the bank line, cross-sectional cut lines, channel centerlines, and secondary flow channel of the river as polylines and then stored them in a geo-database.

Those digitized and georeferenced land-sat images were used to identify morphological changes (used for Planform change detection) in the recent past, from 2010 to 2020, which were then compared to the changes based on classified features. Planform Change detection is the technique of identifying alterations in an object or phenomenon's state through repeated observation at different times for investigating the change in surface phenomena on the earth [11].

In this study, different planform metrics such as Braidedness index, Sinuosity, and width-to-depth ratio are used to detect planform change.

Width-to-depth ratio (w/d): The width-to-depth ratio, which is the ratio of bank-full channel width to bank-full mean depth, and indicates the dimension and shape factors [12]. The width of the river is defined as the point on either side of the river where floodplain vegetation starts and it was estimated by measuring the length of the digitized cross-sectional cut lines or measured from the top width of the provided cross-sections at the endpoint of floodplain vegetation on either side or using satellite sensor data of a single season of a certain year. Whereas the depth was measured from field measurement so that the lowest point measured in the riverbed is taken as bank-full depth. Therefore, the average bank full width, bank full depth, and width-to-depth ratio (w/d) for the years 2010, 2015, and 2020 were estimated for the Mersa river reach (Table 4).

Year	2010	2015	2020
Average bank full-width	99.002m	118.509m	155.423m
Average bank full-depth	1.985m	2.347m	3.014m

Table 4. Bank full width and depth for the three study years of the Mersa river reach.

Sinuosity: Sinuosity is described as the ratio of stream length to valley length [13].

$$Sinuosity=L_{c\ max}/LR$$

Where, L_{cmax}=is the maximum length of the midline of the channel (in single-ch annel rivers), or the widest channel (in multi-channel rivers)

LR=is the overall air length of the reach.

As a result, for this particular study, the overall air length of the reach was fixed from the length of the study reach and the midline of the channel's length was digitally determined from the image of each year. Therefore, the measured result was 2349.811 m, 2330.877 m, and 2553.868 m for the years 2010, 2015, and 2020 respectively. The overall length of the study reaches estimated to be 2103.68 m.

The Braidedness Index (BI): Braiding is explained as a measure of the multiplicity of channels and the new term braid-channel ratio (B) [13].

$$BI=L_{C\ tot}/L_{c\ max}$$

Where, $L_{C\ tot}$=The sum of the mid-channel lengths of all the channels in a reach.

$L_{c\ max}$=The maximum length of the midline of the channel (in single-channel rivers), or the widest channel (in multi-channel rivers).

Therefore, the midline of the channel length and the total length of the mid-channel length of all channels are digitized and calculated from the image of each year. The widest channel length was calculated above and the total mid-channel length for the three study years was estimated to be 2730.48 m, 2906.60 m, and 3751.63 m respectively.

Development of hydrological modeling using SWAT

Watershed delineation: The Watershed delineation procedure is the first step in the SWAT model setup, the Arc SWAT automatic watershed delineation tool was used to create a stream network, define sub-basin outlet locations, delineate the watershed, and calculate the sub-basin parameters. By selecting the minimum threshold value of the drainage area suggested by the Arc SWAT user the stream network definition and sub-watershed size were determined. In this study, the threshold area of 300 ha was taken and the watershed outlet was created manually for finalizing the watershed delineation. So the model delineates a watershed in an area of 53.544 km2 which has 11 sub-basins. The delineated watershed and its twenty-five sub-basins are represented in Figure 8.

SWAT model set up: The data preparation, Watershed delineation, HRU definition, Parameter sensitivity analysis, calibration, and validation were involved in the SWAT model setup Based on the Digital Elevation Model (DEM). Based on land use, soil type, and slope, the watersheds were divided into 11 sub-watersheds and further divided into a total of 84 Hydrologic Response Units (HRUs). to estimate surface runoff from precipitation summed across all the HRUs in a sub-watershed based on soil and land uses/cover the modified Soil Conservation Service (SCS) curve number method was used, and the Penman-Monteith method was used for estimating potential evapotranspiration, while Muskingum method was to simulate channel runoff routing. Finally, the model was run for the years 1997 to 2013 by fixing two years' warm-up period.

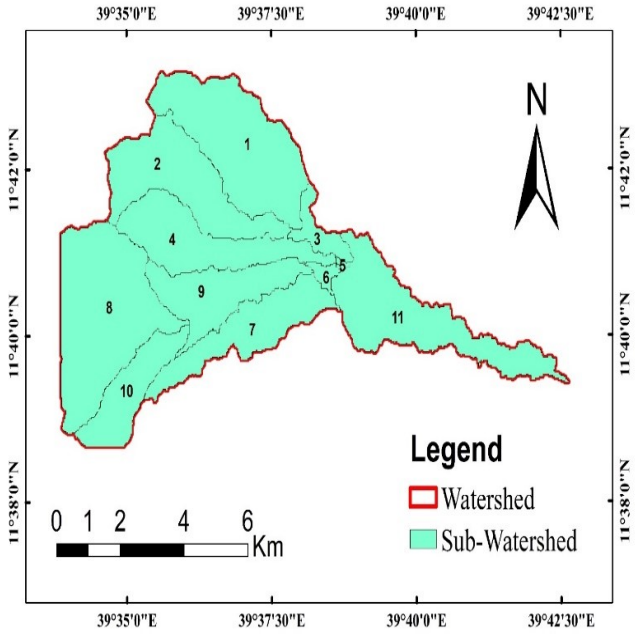

Figure 8. Delineated watershed and its 11 sub-watersheds.

Land use and land cover mapping: Agriculture expansion and rapid population growth affect the land use and land cover pattern of the watershed. The study area land use-landcover map was obtained from the Ministry of Water, Irrigation, and Energy (MoWIE). Land use and land cover data of the study area are prepared as the requirement of the SWAT model and reclassified using the SWAT2012 land use database. There are nine land use/land cover classes dominated by shrubland and Agricultural Land-Generic, which cover about 37.45% and 32.46 of the watershed area respectively, followed by shrubland and agricultural land-generic the deciduous needleleaf forest cover about 15.62% of the area. Range-Brush, Eucalyptus, grass, Urban, and forest covered the remaining area of the watershed (Figure 9 and Table 5).

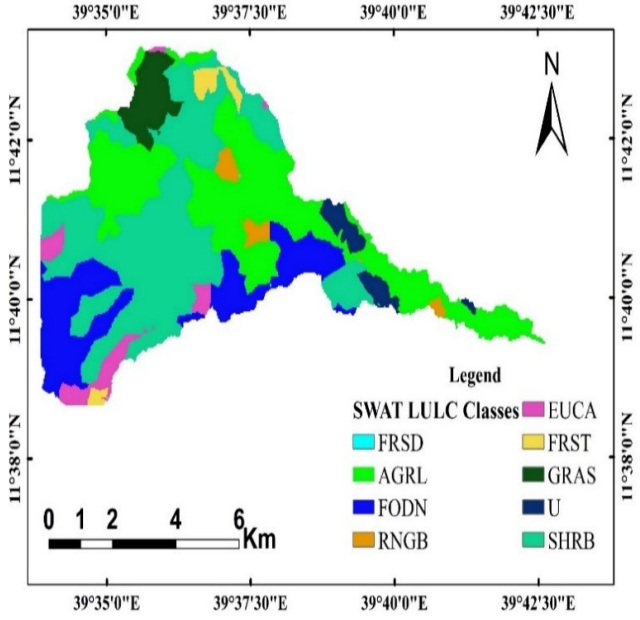

Figure 9. Land use/cover of the watershed as redefined by SWAT code.

Original Land use/cover	SWAT redefined Land use/cover	SWAT code	Area (ha)	% of watershed area
Acacia	Forest-deciduous	FRSD	0.88	0.02
Agricultural land	Agricultural land-generic	AGRA	1738.31	32.46
Dispersed acacia	Deciduous needle leaf forest	FODN	836.31	15.62
Dispersed shrub	Range-Brush	RNGB	97.8	1.83
Eucalyptus	Eucalyptus	EUCA	196.86	3.68
Forest	Forest-mixed	FRST	89.91	1.68
Grass land	Grass land	GRAS	240.01	4.48
Settlement	Urban	U	149.32	2.79
Shrub land	Shrub land	SHRB	2005.01	37.45

Table 5. The original and the redefined land use/cover classes of the Mersa watershed.

Soil mapping of the Mersa watershed: The study area soil map was obtained from the MoWIE GIS department. A soil map is needed for the SWAT model to define HRUs. To integrate the soil map within the SWAT model, it is necessary to make a user soil database that contains the physical and chemical properties required by SWAT models such as available water content, soil texture, hydraulic-conductivity, bulk density, and organic carbon content for the different layers of each soil type in the study area. There are five different soil classes dominated by Eutric-Regosols (32.46%) followed by Leptosols (32.37%). Figure 10 and Table 6 show the Soil map of the watershed as redefined by the SWAT Code and its coverage area

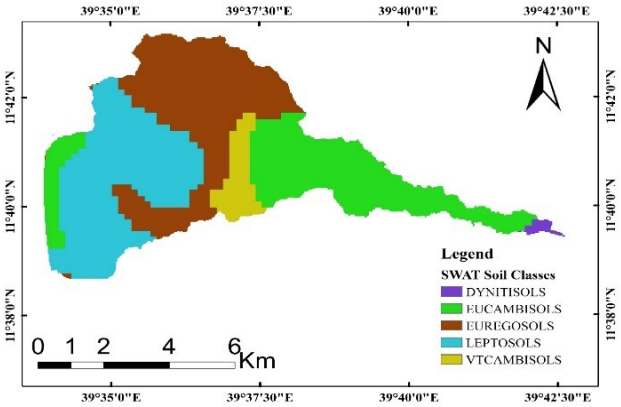

Figure 10. Soil map of Mersa watershed as redefined by SWAT code.

Soil name	SWAT code	Area (ha)	% of watershed area
Dystric nitisols	DYNITISOLS	90.98	0.68
Eutric cambisols	EUCAMBISOLS	3817.44	28.85
Eutric regosols	EUREGOSOLS	4294.26	32.46
Leptosols	LEPTOSOLS	4282.7	32.37
Vertic cambisols	VTCAMBISOLS	745.68	5.62

Table 6. The major soil classes of the Mersa watershed and its area coverage.

Slope and HRU definition: In addition to land use/cover and soil classes, slope classes are also required in HRU analysis in Arc SWAT. For this study, a multiple slope class was selected and classified the slope class into five classes. Therefore, the slopes of 0–3%, 3–8%, 8–15%, 15–30%, and >30% were selected for HRU definition of the study of the Mersa watershed. Table 7 and Figure 11 show the SWAT model slope classification of the watershed. Finally, HRU definition analysis was performed to assign a unique value for each unit in the sub-basin after importing and loading the soil, land cover, and slope data in SWAT projects. For this study, multiple HRU definition options were selected with a default settings threshold of 20%, 10%, and 10% for land use/cover, soil, and slope respectively of individual sub-watershed areas were used. Overall, there were 84 HRUs defined in the entire watershed within 11 sub-watersheds.

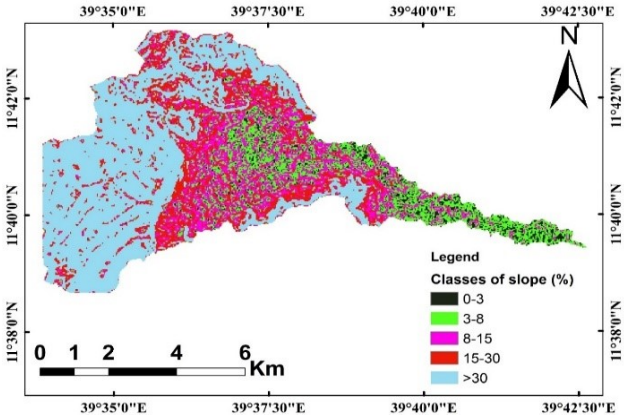

Figure 11. Slope map of Mersa watershed.

Slope (%)	Area (ha)	% of watershed area
0-3	213.81	3.99
3-8	789.3813	14.74
8-15	916.3018	17.11
15-30	931.4972	17.41
>30	2503.441	46.75

Table 7. SWAT model slope classification of the watershed.

Parameter sensitivity analysis: The selection of sensitive parameters is the prerequisite for the calibration and validation of the model. The SWAT model-sensitive parameters were identified and calibrated using a Sequential Uncertainty Fitting version 2 algorithm (SUFI-2) in the SWAT-Calibration and Uncertainty Program (SWAT-CUP) which uses the global sensitivity design method. To improve simulation results and understand the behavior of a hydrological system in the watershed, sensitivity analysis was conducted using 17 stream flow parameters.

Model calibration and validation: Calibration and validation of a hydrological model are required before the model can be used in practice for a specific application. Model calibration is the process of adjusting selected model parameter values and other variables in the model in order to match the model outputs with the observed values, and also model validation is the process of testing the model's ability to simulate observed data. In this study, The SUFI-2 algorithm was chosen over the other algorithms because it is a widely used tool for combined calibration and uncertainty analysis of the SWAT model. The SWAT model was calibrated and validated for Monthly stream flow at the outlet of the watershed (discharge records from 1999 to 2008 were used for calibration and the remaining from 2009 to 2013 were used for validation).

Model performance evaluations: Model evaluation is an essential measure to verify the performance of the model. The performance of the model was evaluated by using statistical measures to determine the quality and reliability of prediction when compared to observed values. In this study, three model evaluation statistics were used to quantify the goodness of fit. Those are coefficient of determination (R^2), Nash-Sutcliffe Efficiency (NSE), and Bias (PBIAS) (Table 8).

Performance	R2	NSE	PBIAS
Very good	$0.75<R^2 \leq 1.0$	$0.75<NSE \leq 1.0$	$PBIAS \leq \pm 10$
Good	$0.60<R^2 \leq 0.75$	$0.60<NSE \leq 0.75$	$\pm 10 \leq PBIAS$
Satisfactory	$0.36<R^2 \leq 0.60$	$0.36<NSE \leq 0.60$	$\pm 15 \leq PBIAS< \pm 25$
Bed	$0.25<R^2 \leq 0.50$	$0.00<NSE \leq 0.36$	$\pm 25 < PBIAS \leq \pm 50$
Inappropriate	$R^2<0.00$	NSE<0.00	$\pm 50 \leq PBIAS$

Source: Adapted from 14-18.

Table 8. The general performance evaluation criteria for recommended performance evaluation measures.

Development of hydraulic model using HEC-RAS

The Hydrologic Engineering Center's River Analysis System (HEC-RAS) model was developed by the United States Army Corps of Engineers Hydrology Engineering Center (HEC). The well-tested HEC-RAS model is widely used for calculating and analyzing one-dimensional steady-flow, predicting water surface profiles in unsteady flow, and estimating the potential for erosion and sediment transport. In this study, HEC-RAS software was used to produce water surface profiles for both steady Gradually Varied Flow (GVF) and unsteady flow conditions, and also a 1-D HEC-RAS model was used to calculate sediment transport capacity and to predict the riverbed change by applying the available sediment balance equations. This model required cross-sections, hydraulic manning roughness, steady flow data (streamflow data output from SWAT), and stream centerline as input parameters to set up and run the model.

Steady flow analysis: For computing, the water flow surface profile the equation used is the energy equation, which is called the direct standard step method from one cross-section to the other cross-section that is solved by an iterative procedure.

$$Z_2+Y_2+(\alpha_2 V_2^2)/2g=Z_1+Y_1+(\alpha_1 V_1^2)/2g+h_e$$

Where:

Z_1, Z_2=bed elevation of the channel at sections 1 and 2 respectively (m)

Y_1, Y_2=water depth at sections 1 and 2 respectively (m)

V_1, V_2=average velocity at sections 1 and 2 respectively (m/s)

α_1, α_2=velocity weighting coefficient at sections 1 and 2

h_e=energy head loss between sections 1 and 2 (m), which is comprised of frictional loss and contraction/expansion loss.

Also, the water discharge is computed in the model using the Manning equation as follows

$$Q=1/n\ A\ R^{3/2}\ S_f^{1/2}$$

Where: Q=Water discharge (m^3/s)

A=Area cross-section (m^2)

R=Hydraulic radius (m)

n=Manning roughness coefficients

The HEC-RAS program used the survey collected cross-section data to establish a 1D steady flow simulation for different discharge scenarios to analyze the water level in all reach of the river. Around 47 cross-sections were collected along the main river reach. A certain range of frequency of discharge magnitude is used for input to the model as upstream boundary conditions. Those discharges used for the upstream boundary conditions study reach are given in Table 9

below from 2 to 100 years return period. The downstream boundary condition is the normal depth which is determined from the longitudinal slope of the river reach. The parameters of the estimated roughness coefficient and nine-year monthly maximum discharges from 2005-2013 were used for model calibration and validations. To calibrate the model, the first six-year discharges from 2005-2010 were used and the rest from 2011-2010 were used for validations.

Return period (year)	Discharge (m^3/s)
2	37.5
5	54.8
10	66.2
25	80.6
50	91.3
100	102

Table 9. Discharge for upstream boundary conditions for the steady flow analysis.

Quasi-unsteady flow (Sediment transport) analysis: Quasi-unsteady flow is used to simulate the sediment analysis or river bed change of the channel. The daily discretized flow records and daily temperature are required in quasi-unsteady sediment transport analysis. For this study, the 9-year daily flow events from 2005 to 2013 out of 17-year recorded flow data and 9-year average daily temperature data from 2005 to 2013 out of 21-year daily temperature data of Mersa were used for analysis and modeled for the sediment simulations. There are different sediment transport equation functions to compute the outflow sediment load. Out of those, Yang and Meyer-Peter Muller's equation for the bed-material load was chosen for sediment analysis for this research.

The 9-year daily instantaneous flow series from 2005 to 2013 were input as external boundary conditions for the upper study reach whereas the SWAT model output sediment load series data were used as downstream boundary conditions for sediment transport analysis in the HEC-RAS model. The flow is discretized into a series of steady flow histograms with a given duration of 24 hours. Similarly, the quasi-unsteady flow also needs temperature boundary conditions, which should have the same length of time as the quasi-unsteady flow series boundary conditions. Therefore, the mean daily temperature record from 2005 to 2013 was inputted into the model and a series of plots were prepared.

Results and Discussion

Data quality analysis result

Consistency test: The quality of data was checked in the data consistency test by using the double mass curve to adjust inconsistently recorded rainfall data. The annual cumulative rainfall for each station and annual mean cumulative rainfall for all stations was linear and the coefficient of determination was very well, as a result of the double mass curve the data was consistent.

Homogeneity test: Non-dimensional plot (graphical relative homogeneity) analysis was used to test the homogeneity of the annual rainfall time series in the watershed. The result of the test, clearly showed that the data values for each station of the watershed were homogeneous and independent. Because the data does not depend on the other stations and graphically all stations do not overlap each other, rather they have similar patterns.

SWAT model results

Parameter's sensitivity analysis: To find the sensitivity order of stream flow to the input parameters, a sensitivity analysis was carried out. The input parameters can be either manually adjusted or accessed in the SWAT-CUP (Calibration and Uncertainty Programs). The SWAT-CUP with SWAT model was set up by considering seventeen parameters for the analysis of sensitivity. 500 simulations were run with SUFI-2, and sensitivity analysis with monthly flow data from 1999 to 2008 was run using global sensitivity analysis. The t-stat offers a measure of sensitivity in the global sensitivity analysis; the largest absolute value shows higher sensitivity, and the p-value determines the significance of sensitivity; a value close to zero has more significance [14]. By considering this result, twelve critical parameters have been identified in the global sensitivity analysis due to their control over the hydrological processes of the examined area. However, SCS Curve Number II (CN2) and Lateral flow travel time (LAT_TTIME) were found to be the most crucial than other parameters for the Mersa watershed (Table 10).

S/no	Parameter name	Description	Min-value	Max-value	Fitted-value	t-stat	p-value
1	R__CN^2.mgt	Initial curve no. at moisture condition II	-0.25	0.25	0.22	51.06925	0

2	V__LAT_TTIME.hru	Lateral flow travel time	0.25	120.3	8.05	-32.1696	0
3	V__ESCO.hru	Soil evaporation compensation	0	1	0.98	12.62758	0
4	R__SOL_Z(..).sol	Soil depth	-0.25	0.25	0.24	-5.99319	0
5	R__SOL_AWC(..).sol	Available water capacity	-0.25	0.25	-0.19	-5.794	0
6	V__RCHRG_DP.gw	Deep aquifer percolation fraction	0	1	0.08	-5.26895	0
7	V__GW_DELAY.gw	Groundwater delay	0	500	137.5	-4.29786	0.000021
8	R__SOL_K(..).sol	Saturated hydraulic conductivity	-0.25	0.25	0.22	1.935282	0.05354
9	V__ALPHA_BF.gw	Base flow alpha fact	0	1	0.08	1.041254	0.29828
10	V__ALPHA_BNK.rte	Baseflow alpha factor for bank storage	0	1	0.69	0.918551	0.35879
11	V__EPCO.hru	Plant uptake compensation factor	0	1	0.65	-0.69679	0.486273
12	V__REVAPMN.gw	Threshold water depth in the shallow aquifer	0	500	439.5	-0.63703	0.524406

Table 10. Flow-sensitive parameter and fitted value.

Calibration and validation of SWAT model: The calibration and validation were done for sensitive flow parameters of SWAT with observed average monthly discharge data. Model calibration testing the model with known input and output data involves making certain parameter adjustments, while validation involves a comparison of the model results to an independent dataset during calibration without the calibration parameters being adjusted further flow predictions were calibrated using 1999 to 2008 monthly flow data and validated using 2009 to 2013 monthly flow data using the SUFI-2 algorithm. According to the model performance evaluation given by Moriasi DN, et al. [15], the calibration results of the SUFI-2 program summarized the value of the correlation coefficient (R^2), Nash-Sutcliffe Simulation Efficiency (NSE), and percent of bias (PBIAS), which were used as the main objective functions for the model following the SUFI-2 approach between the observed and predicted stream flow. Based on the results of these studies, the Coefficient of determination, Nash Sutcliffe coefficient, and percentage of bias were 0.78, 0.75, and 21.6 for the calibration period, respectively, and 0.80, 0.77, and 19.16 for the validation period (Figures 12 and 13).

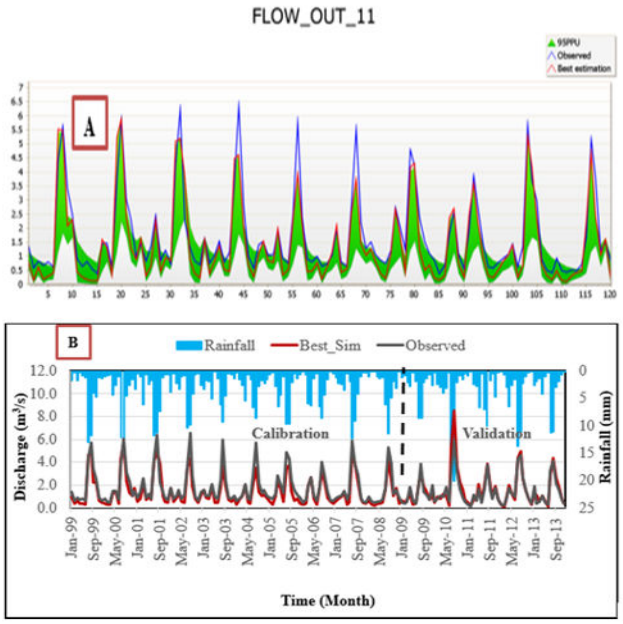

Figure 12. Calibration and validation result of monthly simulated and measured flow at the watershed outlet.

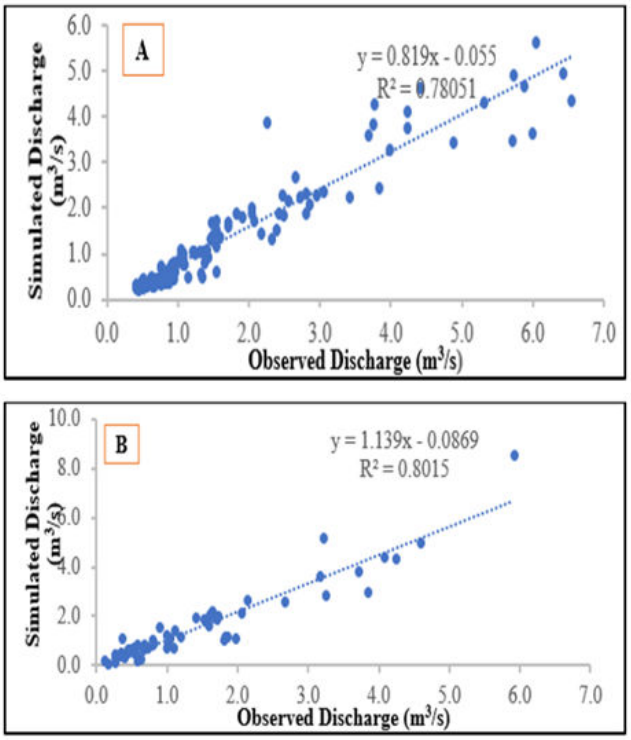

Figure 13. The regression coefficient of monthly calibration (A) and validation (B) of discharge in the outlet of the Mersa watershed.

River bed and bank conditions

By examining the samples of collected bed material, river bed, and bank compositions were investigated with the laboratory results of the soil gradation curve and the *in situ* conditions. The percentage of fine sand, coarse sand, and gravel coverage was 22.02%, 14.06%, and 63.64%, the rest of 0.98% is fine grain soil for upper Mersa bed material gradation and 32.01%, 18.63%, and 48.02% respectively, the rest 1.34% covers fine-grained soils for lower Mersa bed material gradation. The result indicated that coarse-grained soil was dominated by sand (fine sand to very coarse sand) and gravel (from very fine gravel to medium gravel) with a Uniformity coefficient (D60/D10) of 27.06 and 15.64 for upper and lower bed material, these higher values of uniformity coefficient show that a moderately sorted and a well-graded coarse-grained soil.

Similarly, the percentage value of gravel, coarse sand, fine sand, and fine-grained soil (silt and clay) is estimated to be 3.74%, 6.13%, 39.24%, and 50.89% respectively for the lower bank. Also 21.51%, 11.15%, 26.08%, and 41.26% respectively for the upper bank. This indicated that the bank material was dominated by fine-grained soils of silt and clay with a size smaller than 0.075 mm. Depending on the percentage of the gravel, sand, and fine-grained soil in the soil material; we can categorize the bank soil materials as silt loam or clay loam due to the percentage of silt and clay in the bank materials. The characteristics of D90 particle size are estimated as 4.75 mm at which 90% of the soil is finer than this size. The grading often follows a fine-grained soil gradation. Upper Mersa bank has a lower percentage of fine-grained soil than lower Mersa bank. This may be due to sediment intake from the eroded channel, an increase in discharge downstream, which decreases flow velocity, and a widening of the downstream section of the river reaches, which causes more sediment to be deposited on the bed and banks.

Planforms quantitative analysis

There are various ways of assessing a river's morphological change, in this study, a planform metrics method was used to detect and identify the morphological changes of Mersa River. The planform metrics (width-to-depth ratio, Sinuosity, Braidedness index,) of the sequential planform maps generated from the time-series data for each year were used for a quantitative analysis of the planform change.

Width-to-depth ratio: It is measured from the ratio of bank-full width to a maximum depth of the thalweg, which is an indicator of morphological change delineation of natural rivers. In this study for the main Mersa river, the width-to-depth ratio shows that the value is almost greater than 40 m/m for the whole station cross-sections. Those values are 49.88, 50.49, and 51.57 for the years 2010, 2015, and 2020 respectively. The width-to-depth ratio shows an increasing trend that indicates the width of the river reach is increasing regardless of the depth [16]. This increase in width causes the riverfront bank to retreat, resulting in land loss and property damage Therefore, according to Rogen's classification, Mersa river reach is classified as D-stream types based on this criterion and the ranges of values used for delineations.

Sinuosity: sinuosity is a method of classifying natural rivers based on range. For this study, sinuosity was measured for the three study years. Then the measured sinuosity for the years 2010, 2015, and 2020 are 1.117, 1.107, and 1.214 respectively (Figure 14). The sinuosity values increased from 2010 to 2020, which implies that the deepest channel's length increased from side to side, which leads to bank erosion and land loss. According to Rogen's classification, this result shows that the main Mersa river reaches classify between the broader classifications of D and DA stream types (Sinuosity value from <1.1 to 1.6).

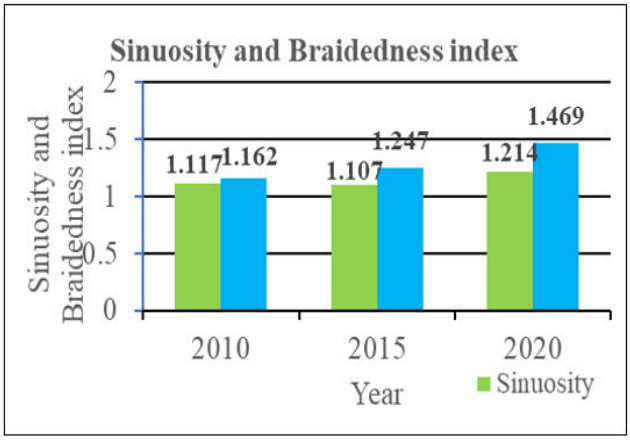

Figure 14. The sinuosity and Braidedness index value of the three years of the Mersa river.

The Braidedness index: It is calculated by the ratio of the sum of the secondary channels to the length of the deepest channel in the reach. As shown in Figure 14 above, the index value for the Mersa river was estimated to be: 1.162, 1.247, and 1.469 respectively, for the years 2010, 2015, and 2020. The Braidedness index shows a value greater than unity and an increasing trend for the three study years. This implies channel multiplicity and formation of bars due to the summation of the length of the secondary channel being greater than the length of the main channel for a fully braided river. This channel multiplicity and formation of bars push the flow towards the bank and it causes bank erosion. This result shows that the river is characterized by increasing braided natures Figure 14 above.

Therefore, the Mersa river reach is classified as a D4-stream type in Rosgen's categorization system based on the result of sinuosity, width-to-depth ratio, and dominant bed material conditions. This classification develops in the level of precision from more broad morphological classification to specific measurable morphological categories. However, based on its width-to-depth ratio, sinuosity results, and conditions for the main bed material, the river reach fits into the category of a shallow, wide, and gravel-bedded stream type. Therefore, the river reach could be sinuous-braided patterns.

Steady flow analysis results

Water surface profile for 2, 5, 10, 25, 50, and 100yrs return period design discharges was calculated in the model using Manning's methods by considering gradually varied flow profiles (direct step iteration method) at each cross-section

According to model results, the 2 yr, 5 yr, and 10 yr design discharge almost accommodated within the flood plain limits in all of the stations of the Mersa river reach. But there is a condition that significant areas adjoining the flood could be flooded by the 25, 50, and 100 yrs design discharges due to which had the small height river bank under one or both banks. For example, in the Figure 15 below the river bank height on the left side was large while the right bank height was small even if the 2-year design discharge was accommodated but for 5, 10, and 25 year return period peak flood discharge the catchment would be flooded at station 45. In the same manner, at station 12 shown below on the left side again because the height of the bank was small, there was an excess flood.

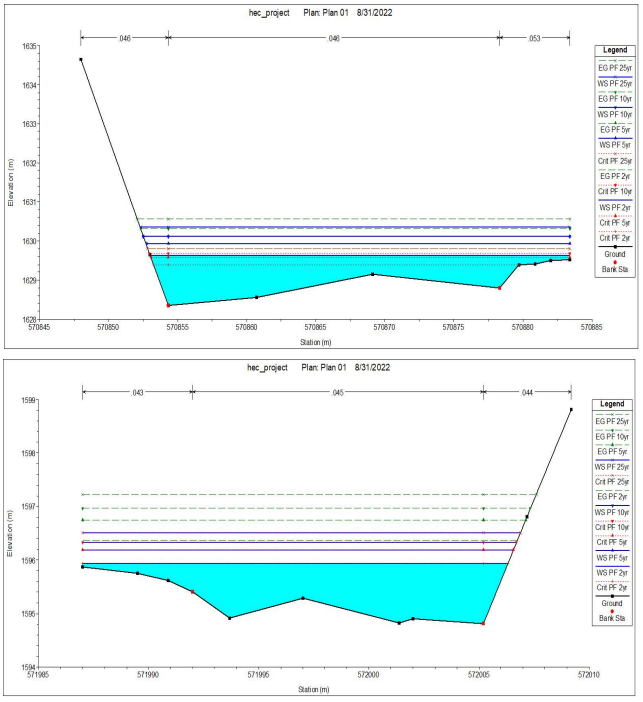

Figure 15. Cross-section plot on river station 12 of Mersa river.

According to the model's predicted result shown in the Figure 16 below flooding for areas with design discharges of 50 and 100 years. The reality also supports the model's predictions, especially for lower reach from station 8 to station 4 where a significant area had been inundated, as illustrated by the model's design discharge results for discharges with 50 and 100-year return periods

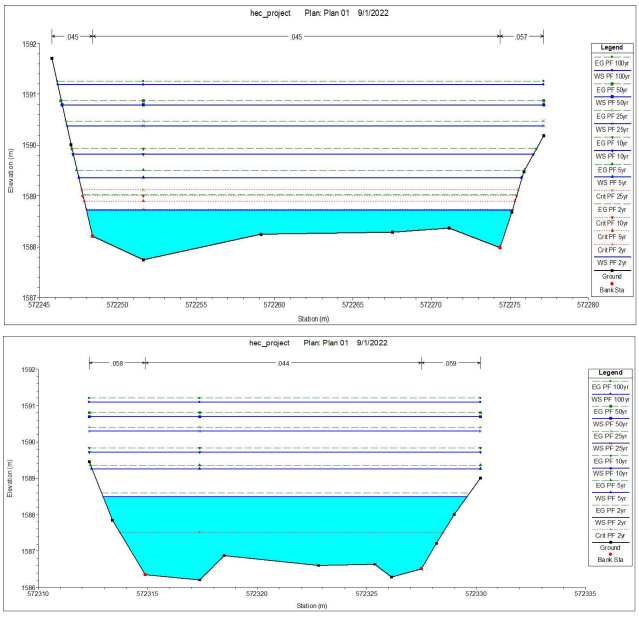

Figure 16. Cross-section plot on river station 5 and station 4 of Mersa river.

Vertical bed change (aggradations and degradation process)

The river reach conducts both aggradations and degradation along the study reach of both the Mersa River. The model was tested by Meyer Peter Muller and Yang for sediment transport functions with 9-year daily flow and temperature data,

According to the Meyer Peter Muller sediment transport formula result was plotted and tabulated as follows the maximum degradation to a depth of 1 m at stations 16, 32, 40, and a maximum deposition of 1.103 m at station 3 was observed. The average degradation and aggradations of the Mersa river reach are estimated to be 0.70 m and 0.66 m respectively. This result indicated that the river reach shows almost a degradation process in all stations except some at the downstream ends (Table 11).

Change of channel invert at start and end of simulations (m)

River	Reach	RS	2005	2006	2007	2008	2009	2010	2011	2012	2013
Mersa	all reach	47	-0.863	-1	-1	-1	-1	-1	-1	-1	-1
Mersa	all reach	46	-0.486	-0.75	-0.75	-0.75	-0.75	-0.75	-0.75	-0.75	-0.75
Mersa	all reach	45	-0.712	-0.629	-0.682	-0.715	-0.715	-0.715	-0.715	-0.715	-0.715
Mersa	all reach	44	-0.955	-0.852	-0.855	-0.855	-0.855	-0.855	-0.855	-0.855	-0.855
Mersa	all reach	43	-0.661	-0.883	-0.889	-0.889	-0.884	-0.884	-0.884	-0.884	-0.884
Mersa	all reach	42	-0.496	-0.794	-0.794	-0.794	-0.794	-0.794	-0.794	-0.794	-0.794
Mersa	all reach	41	-0.338	-0.526	-0.526	-0.525	-0.571	-0.571	-0.571	-0.571	-0.571
Mersa	all reach	40	-1	-1	-1	-1	-1	-1	-1	-1	-1
Mersa	all reach	39	-0.401	-0.69	-0.691	-0.684	-0.684	-0.684	-0.7	-0.704	-0.704
Mersa	all reach	38	-0.465	-0.548	-0.636	-0.636	-0.636	-0.636	-0.626	-0.789	-0.789
Mersa	all reach	37	-0.066	-0.206	-0.253	-0.253	-0.253	-0.253	-0.253	-0.253	-0.253
Mersa	all reach	36	-0.058	-0.242	-0.242	-0.242	-0.242	-0.242	-0.242	-0.242	-0.242
Mersa	all reach	35	0.046	-0.02	-0.038	-0.037	-0.037	-0.037	-0.05	-0.05	-0.05
Mersa	all reach	34	0.001	0.056	0.041	0.041	0.041	0.041	0.042	0.042	0.042
Mersa	all reach	33	-1	-0.994	-0.996	-0.996	-0.996	-0.996	-0.996	-0.996	-0.996
Mersa	all reach	32	-0.995	-1	-1	-1	-1	-1	-1	-1	-1
Mersa	all reach	31	0.158	-0.351	-0.435	-0.435	-0.519	-0.569	-0.6	-0.615	-0.62
Mersa	all reach	30	1.193	0.718	0.706	0.706	0.714	0.716	0.632	0.632	0.632
Mersa	all reach	29	-0.553	-0.75	-0.748	-0.79	-0.79	-0.79	-0.79	-0.79	-0.79
Mersa	all reach	28	-0.811	-0.816	-0.731	-0.745	-0.736	-0.74	-0.743	-0.743	-0.743
Mersa	all reach	27	-0.281	-0.346	-0.378	-0.384	-0.383	-0.383	-0.398	-0.429	-0.429
Mersa	all reach	26	-0.307	-0.461	-0.458	-0.458	-0.458	-0.458	-0.456	-0.457	-0.457
Mersa	all reach	25	-0.658	-0.73	-0.786	-0.792	-0.79	-0.79	-0.774	-0.794	-0.794
Mersa	all reach	24	-0.415	-0.272	-0.268	-0.268	-0.268	-0.268	-0.261	-0.244	-0.263
Mersa	all reach	23	-0.788	-0.827	-0.904	-0.923	-0.795	-0.795	-0.798	-0.856	-0.856
Mersa	all reach	22	-0.783	-0.936	-0.865	-0.865	-0.864	-0.864	-0.872	-0.872	-0.872
Mersa	all reach	21	-0.316	-0.548	-0.58	-0.586	-0.588	-0.588	-0.564	-0.592	-0.592
Mersa	all reach	20	-0.606	-0.81	-0.832	-0.832	-0.831	-0.831	-0.829	-0.834	-0.834

Mersa	all reach	19	-0.413	-0.536	-0.761	-0.799	-0.806	-0.649	-0.638	-0.651	-0.651
Mersa	all reach	18	-0.314	-0.442	-0.483	-0.493	-0.477	-0.477	-0.474	-0.555	-0.554
Mersa	all reach	17	-0.919	-1	-0.997	-0.997	-0.997	-0.997	-0.997	-0.997	-0.997
Mersa	all reach	16	-0.995	-0.981	-1	-1	-1	-0.997	-1	-1	-1
Mersa	all reach	15	-0.418	-0.534	-0.574	-0.574	-0.574	-0.578	-0.574	-0.584	-0.584
Mersa	all reach	14	-0.066	-0.133	-0.136	-0.136	-0.136	-0.136	-0.135	-0.135	-0.135
Mersa	all reach	13	-0.431	-0.541	-0.548	-0.548	-0.548	-0.548	-0.551	-0.551	-0.551
Mersa	all reach	12	-0.981	-0.987	-0.985	-0.985	-0.985	-0.985	-0.985	-0.985	-0.985
Mersa	all reach	11	-0.398	-0.53	-0.591	-0.641	-0.67	-0.677	-0.677	-0.852	-0.852
Mersa	all reach	10	-0.739	-0.856	-0.858	-0.862	-0.862	-0.854	-0.861	-0.861	-0.861
Mersa	all reach	9	-0.555	-0.751	-0.712	-0.731	-0.731	-0.759	-0.773	-0.773	-0.773
Mersa	all reach	8	-0.67	-0.564	-0.632	-0.617	-0.617	-0.596	-0.625	-0.631	-0.631
Mersa	all reach	7	-0.809	-0.332	-0.589	-0.597	-0.611	-0.611	-0.578	-0.708	-0.708
Mersa	all reach	6	-0.742	-0.539	-0.681	-0.571	-0.569	-0.569	-0.568	-0.597	-0.597
Mersa	all reach	5	-0.994	-0.789	-0.754	-0.693	-0.691	-0.758	-0.754	-0.747	-0.747
Mersa	all reach	4	-0.029	0.445	0.775	0.743	0.704	0.584	0.628	0.712	0.665
Mersa	all reach	3	0.254	0.455	0.78	1.028	1.039	1.024	1.039	1.05	1.1
Mersa	all reach	2	0.247	0.865	-0.794	-0.827	-0.807	-0.407	-0.826	-0.823	-0.818
Mersa	all reach	1	0.327	0.328	0.65	0.83	0.685	0.689	0.811	0.85	0.85

Table 11. Bed elevation differences along the bed profile according to Meyer Peter Muller (-ve sign is degradations and +ve sign is aggradation).

In the Meyer Peter Muller, sediment transport results Some cross-section bed change plots show no aggradation or degradation at the left and right bank including the channel bed were observed (Figure 17 A) and also some stations show aggrade or degradation observed at the right and left bank in addition to the channel bed (Figure 17 B-D). In the same manner, there was no deposition or erosion on the river bank whereas the degradation was observed at the channel bed only in some stations.

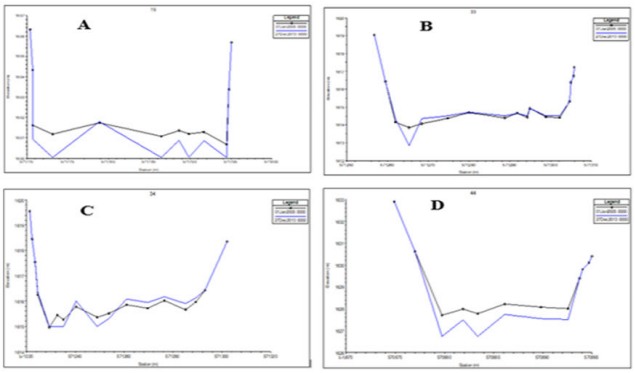

Figure 17. Cross-section bed change plot that shows degradations at stations 19, 33, 34, and 44 (A, B, C, and D) respectively of the Mersa river reach according to Meyer Peter Muller.

In the second scenario, the river reaches were simulated for Nine years' period with Yang's transport functions. According to Yang's sediment transport formula, as we can see from Table 12 below, the maximum degradation to a depth of 0.999 m at stations 32, 16, 12, and 10 respectively, and a maximum deposition of 3.53 m at station 3 was observed. The average degradation and aggradations of the Mersa River reach are estimated to be 0.84 m and 1.42 m respectively [17].

Change of channel invert at start and end of simulations (m)

River	Reach	RS	2005	2006	2007	2008	2009	2010	2011	2012	2013
Mersa	all reach	47	-0.995	-0.995	-0.995	-0.995	-0.995	-0.995	-0.995	-0.995	-0.995
Mersa	all reach	46	-0.824	-0.824	-0.797	-0.797	-0.797	-0.797	-0.797	-0.797	-0.797
Mersa	all reach	45	-0.872	-0.872	-0.872	-0.875	-0.875	-0.875	-0.875	-0.875	-0.875
Mersa	all reach	44	-0.917	-0.921	-0.921	-0.919	-0.919	-0.919	-0.919	-0.919	-0.919
Mersa	all reach	43	-0.937	-0.948	-0.948	-0.948	-0.948	-0.948	-0.948	-0.948	-0.948
Mersa	all reach	42	-0.466	-0.895	-0.895	-0.895	-0.895	-0.895	-0.895	-0.895	-0.895
Mersa	all reach	41	-0.319	-0.668	-0.701	-0.701	-0.701	-0.701	-0.701	-0.701	-0.701
Mersa	all reach	40	-0.194	-0.996	-0.996	-0.996	-0.996	-0.996	-0.996	-0.996	-0.996
Mersa	all reach	39	0.152	-0.697	-0.994	-0.994	-0.994	-0.994	-0.994	-0.994	-0.994
Mersa	all reach	38	-0.077	-0.565	-0.75	-0.94	-0.94	-0.94	-0.94	-0.94	-0.94
Mersa	all reach	37	-0.32	-0.202	-0.403	-0.565	-0.686	-0.798	-0.907	-0.966	-0.996
Mersa	all reach	36	-0.001	0.21	0.303	0.149	0.15	0.184	0.186	0.186	0.186
Mersa	all reach	35	0.141	0.187	0.227	0.182	0.178	0.178	0.19	0.19	0.19
Mersa	all reach	34	-0.764	-0.653	-0.688	-0.475	-0.682	-0.681	-0.68	-0.68	-0.679
Mersa	all reach	33	-0.891	-0.936	-1	-0.995	-0.995	-0.995	-0.995	-0.995	-0.995
Mersa	all reach	32	-0.411	-0.178	-0.376	-0.635	-0.662	-0.906	-0.999	-0.999	-0.999
Mersa	all reach	31	0.04	0.322	0.229	0.119	-0.184	-0.172	-0.302	-0.389	-0.444
Mersa	all reach	30	1.091	1.351	1.284	1.192	0.935	0.945	0.905	0.885	0.879
Mersa	all reach	29	-0.815	-0.751	-0.762	-0.759	-0.766	-0.767	-0.772	-0.771	-0.771
Mersa	all reach	28	-0.851	-0.98	-0.937	-0.882	-0.89	-0.887	-0.8	-0.799	-0.798
Mersa	all reach	27	-0.433	-0.703	-0.695	-0.928	-0.859	-0.753	-0.74	-0.787	-0.746
Mersa	all reach	26	-0.68	-0.926	-0.92	-0.931	-0.921	-0.919	-0.922	-0.926	-0.926
Mersa	all reach	25	-0.277	-0.932	-0.936	-0.935	-0.938	-0.944	-0.946	-0.952	-0.951
Mersa	all reach	24	-0.25	-0.63	-0.689	-0.663	-0.676	-0.683	-0.647	-0.643	-0.64
Mersa	all reach	23	-0.173	-0.729	-0.827	-0.831	-0.836	-0.809	-0.817	-0.816	-0.816
Mersa	all reach	22	0.038	-0.388	-0.689	-0.703	-0.694	-0.769	-0.79	-0.792	-0.798
Mersa	all reach	21	-0.428	-0.598	-0.711	-0.729	-0.731	-0.749	-0.762	-0.767	-0.767
Mersa	all reach	20	-0.692	-0.797	-0.743	-0.799	-0.753	-0.749	-0.754	-0.753	-0.752
Mersa	all reach	19	-0.196	-0.354	-0.65	-0.708	-0.708	-0.72	-0.693	-0.716	-0.712
Mersa	all reach	18	-0.547	-0.595	-0.763	-0.96	-0.966	-0.946	-0.831	-0.892	-0.712
Mersa	all reach	17	-0.264	-0.594	-0.499	-0.672	-0.661	-0.657	-0.726	-0.886	-0.885
Mersa	all reach	16	-0.173	-0.494	-0.913	-0.998	-0.994	-0.998	-0.999	-0.999	-0.999
Mersa	all reach	15	-0.323	-0.48	-0.776	-0.993	-0.981	-0.989	-0.985	-0.996	-0.994
Mersa	all reach	14	-0.323	-0.494	-0.492	-0.908	-0.776	-0.771	-0.696	-0.786	-0.784
Mersa	all reach	13	-0.634	-0.975	-0.979	-0.984	-0.981	-0.982	-0.986	-0.989	-0.993
Mersa	all reach	12	-0.577	-1	-0.998	-0.999	-1	-1	-1	-0.999	-0.999

Mersa	all reach	11	-0.54	-0.624	-0.833	-0.925	-0.817	-0.812	-0.771	-0.794	-0.804
Mersa	all reach	10	-0.841	-0.65	-0.814	-0.999	-0.996	-0.996	-0.999	-0.999	-0.999
Mersa	all reach	9	-0.34	-0.09	-0.107	-0.454	-0.505	-0.729	-0.731	-0.753	-0.802
Mersa	all reach	8	-0.235	0.237	0.256	-0.003	-0.146	-0.227	-0.203	-0.277	-0.328
Mersa	all reach	7	-0.126	0.758	0.8	0.804	0.765	0.3	0.349	0.311	0.264
Mersa	all reach	6	0.128	1.119	1.042	0.844	0.636	0.565	0.257	0.608	0.598
Mersa	all reach	5	0.628	0.825	0.925	0.935	1.224	1.379	1.412	1.444	1.462
Mersa	all reach	4	1.363	1.816	2.186	2.338	2.478	2.571	2.593	2.663	2.72
Mersa	all reach	3	2.449	3.045	3.373	3.44	3.396	3.572	3.595	3.5	3.531
Mersa	all reach	2	2.411	1.696	2.275	1.867	1.731	1.756	1.694	1.724	1.718
Mersa	all reach	1	0.885	1.98	2.222	2.597	2.829	2.877	3.006	2.595	2.608

Table 12. Bed elevation differences along the bed profile according to Yang's (-ve sign is degradations and +ve sign is aggradation).

Similarly, In Yang's sediment transport result some cross-section bed change plots show no aggradation or degradation at the left and right banks including the channel bed were observed and also some stations show aggrade or degradation observed at the right and left banks in addition to the channel bed. In the same fashion, there was no deposition or erosion on the river bank whereas the degradation was observed at the channel bed only in some stations.

Additionally, field observations and survey data collection were conducted in May of 2022, one year later in reference to a common datum with the 2021 surveyed cross-sections at stations 6, 7, 8, 14, 15 18, 19, 33, 34, 40, and 41) in both the lower and upper river reach's and then measured the vertical and horizontal distance in the middle of the channel and toe of the bank as shown below. This measured value represents the vertical aggradation/degradation and bank erosion for the last year. We have seen in the Figure 18 below for the last year the study reach shows almost similar trends of aggradation and degradation with the model simulation results.

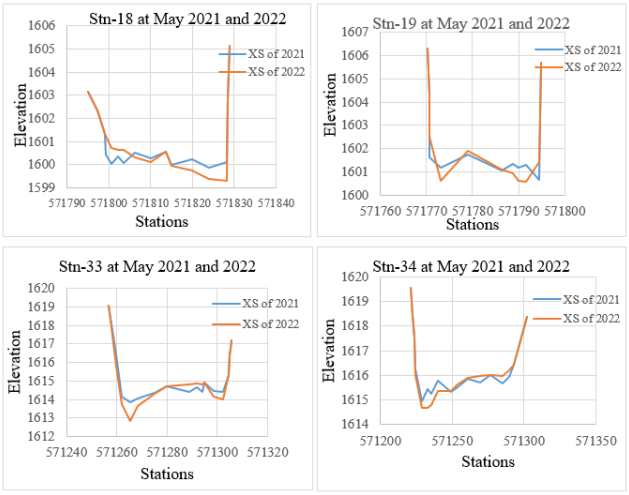

Figure 18. The old (2021) and new (2022) cross-section comparison at stations 18, 19, 33, and 34 of the lower and upper river reach.

To select the appropriate one from the two scenarios (Yang transport method and Meyer Peter and Muller transport method) the field observation and sample Cross-section surveyed after one-year later on May 2022 (the same benchmark as before 2021) were taken to compare the two methods model results. The one-year later surveyed cross-section differencing results of aggradation and degradation and the one-year simulation result of the Yang and Meyer Peter and Muller transport formula is tabulated as follows in Table 13 below.

Transport	Main Mersa river	
Formula	1-year simulation result	
	Aggradation (m/yr.)	Degradation (m/yr.)
Meyer peter muller	0.073	0.078
Yang	0.157	0.093
1-year later collected survey	0.062	0.081

Table 13. Comparing simulation results of different transport functions and field observations.

As compared to the practical expected bed elevation changes simply judged by field observation, the Meyer Peter Muller looks to work better with the Mersa study reach degradation and aggradation trends, whereas, it better works the depth of aggradation and degradation for the Mersa river reach and can effectively be used for analysis and design.

According to the field observations (the 2021 and the one-year later 2022 surveyed cross-section differencing) results, the maximum average aggradation for the Mersa study reach was not greater than 0.062 meters per year, and the maximum average degradations were not greater than 0.081 meters per year. This demonstrates that Meyer Peter Muller's simulation results and the field observation results have a good level of agreement. In comparison to Yang's transport function results for the study reach, the simulation results of Meyer Peter Muller's transport function generally produce approximately realistic vertical changes. As a result, the river reaches are accurately represented by the Meyer-Peter-Muller transfer formula [18].

As indicated by this research analysis outcomes, the Mersa river reach undergoes seasonal changes in degradation and aggradations at the same time due to the following different reasons. (I) The river reaches aggrade and/or degrades simultaneously, and the aggraded part pushes the flow to the degraded parts, which results in a seasonal change in the river's flow direction. (II) The river at a given cross-section erodes completely but in various intensities along the cross-section stationing, which creates more flow to the highly eroded areas and subsequently leads to shifting of the flow channel to these areas and leaves the other part as aggraded. (III) The river reaches at the specified station completely aggrades, but within varying intensities along the cross-section stationing, which increases flow to the lowly aggraded areas and, as a result, it causes for shifting of flow.

Generally, the result of this study showed that the Mersa river reach is in the degrading process, especially at the upstream study reach. and aggradation also along the study reach especially at the downstream study reach [19].

Protective measures to be taken for beds and banks of the river

To apply various forms of protective measures for river erosion and instability, it is required to determine the type of failure in the field, either scouring or shear failure. In this study, the materials that make up the river's bed and the bank have very little resistance against the erosive forces produced by the flow. Therefore, this process of aggradations and/or degradations and channel shifting needs to be stabilized. This was achieved by providing appropriate hydraulic structure construction. The masonry retaining wall, concrete wall, gabion wall, etc. are used as stabilized structures to protect flood areas from flooding and to control the failure of river banks. Whereas the vertical bed stability was enhanced by constructing grade control structures or transversal structures (such as check dam and drop structures) perpendicular to the flow direction to lower the river's longitudinal slope, reduce flow velocity, and reduce and control the local channel width.

Conclusion

The morphological change of rivers due to complex scouring and deposition processes is one of the main characteristics of natural rivers. This could result from changes in river sediment transport and flow conditions. Hence, this study investigates the morphological change of the Mersa river, which has a condition of river bank failure and as a result, the river has been caused for losing the farmer agricultural land, properties, and any hydraulic structure such as bridges. This investigation has been done by analyzing the vertical and horizontal change of the study river reach and quantifying the subsequent bank erosion. As a result of this aggradation-degradation process, sediments are deposited or eroded on/from the riverbed in a spatially variable pattern along the river reach, which elevates or lowers the riverbed, this process leads to an increase in lateral migration rates, width to depth ratios, and over bank flooding (flood inundation). Therefore, the HEC-RAS Model simulation result demonstrated that the study river reach shows vertical adjustments of aggradation (0.159 m/y) and degradation (0.078 m/y) for the main Mersa study reach.

This study also detects the planform changes and investigates the river morphology changes based on the multi-temporal images of Landsat over the entire years of 2010, 2015, and 2020 by exploring different morphological metrics parameters, such as sinuosity index, braiding index, and river width to depth ratios. Those morphological metrics parameter values are slightly increased from 2010 to 2020. The width-to-depth ratio result shows an increasing trend which means the width of the river increases irrespective of the river depth Due to bank erosion, as a result, the river becomes widening and shallower because wide channels are produced by lateral erosion. The

increasing trend of the Braidedness index also demonstrates the development of island/bar area formations, which causes the flow to be pushed to both sides of the banks and the increasing sinuosity value shows that the increasing thalweg length of the study reaches from year to year which leads to lateral retreat. This lateral retreat (bank erosion) and vertical bed changes harmed agricultural land, properties, and any hydraulic structure along the riverside.

Generally, the studied Mersa river reach continued to undergo morphological changes over the entire period between 2010, 2015, and 2020 for which historical photographs were available due to seasonal variation of aggradation and degradations that resulted from flow and sediment discharge in the river which caused for losing the farmer agricultural land, properties, and any hydraulic structure near and around the river.

Recommendations

Based on the findings, key morphological changes in the river reach included a combination of river bank erosion, vertical bed change, and channel widening or lateral displacement of the active channel, which leads to damaged properties, and any hydraulic structure and loss of lands near and around the river. Therefore, this study recommended that appropriate conservation measures should be implemented to control the failure of river banks and river vertical bed changes and to prevent the study reach from further land loss and other damage.

Due to the availability of materials like sand, gravel, stone, and boulders are sufficient the stabilization structure can be a masonry retaining wall, concrete wall, and gabion wall were selected but due to cost vertical gabion bank is recommended to control river bank erosion instabilities Mersa river, and also the provision of the Transversal protection structures (grade control structure) Check dam and drop structures are recommended to control the vertical bed change of Mersa river.

The Stream flow data used for this study were older (up to 2013) due to this the design flood did not present the current situation on the study channel. Therefore, the satellite images of the years 2010, 2015, and 2020 were digitized whereas sinuosity, Braidedness index, and the width-to-depth ratio were calculated to investigate the planform changes and to represent the current situations of the river.

Sediment data in this study area were not sufficient to conduct the research, so the SWAT model output sediment data was used without modification for sediment transport analysis.

Declarations

The authors declare no conflict of interest.

Availability of Data and Materials

The data used and analyzed in the current study are available from the corresponding author on reasonable request.

Author Contribution

Yonatan Tibebu Ayele and Dr. Fikru Fentaw Abera designed the technical route of the study, analyzed the data, and wrote the manuscript. Hussen Ali Hassen Ayana and Yohannes Wodaje proposed suggestions to improve the quality of the manuscript. The author has read and agreed to the published version of the manuscript.

Code Availability

Software codes are available from the corresponding author on reasonable request.

Funding

The authors did not receive support from any organization for the submitted work.

Ethics Approval

Not applicable.

Consent to Participate

Informed consent was obtained from all individual participants included in the study.

Consent for Publication

Not applicable.

References

1. Chinnarasri, Chaiyuth, Tawatchai Tingsanchali, and Surakai Banchuen. "Field validation of two river morphological models on the Pasak River, Thailand." *Hydrol Sci* J 53 (2008): 818-833.
2. Richardson, Everett V, Daryl B. Simons, and Peter Frederick Lagasse. River engineering for highway encroachments: Highways in the river environment. No. FHWA-NHI-01-004. United States. Federal Highway Administration, 2001.
3. Simons DB. "The geomorphic and hydraulic response of rivers." Arizona-Nevada Academy of Science, 1975.
4. Richards, Mariah. "Braided river response to eight decades of human disturbance, Denali National Park and Preserve, AK." Master's thesis, Colorado State University, 2016.
5. Sevruk B, M Ondras, and B Chvíla. "The WMO precipitation measurement intercomparisons." *Atmos Res* 92 (2009): 376-380.
6. Chow, Ven Te. "Open channel flow." London: McGRAW-HILL 11 (1959): 99-136.
7. French, Richard H, and Richard H. French. "Open-channel hydraulics." New York: McGraw-Hill, 1985.

8. Arora K. "Soil mechanics and foundation engineering in SI units." 1992: Standard publisher's distributors. (1992).

9. Dahmen ER, and Michael John Hall. "Screening of hydrological data: tests for stationarity and relative consistency." 49 (1990).

10. Subramanya K. "Engineering Hydrology. McGraw-Hill Education (India) Private Limited." New Delhi (2013).

11. Mahmud-ul-Islam, Syed. "Land use change detection of the Buriganga River using GIS tools and its water management for promoting a sustainable environment." (2011).

12. Rosgen, David L. "A classification of natural rivers." *Catena* 22 (1994): 169-199.

13. Friend PF, and Rajiv Sinha. "Braiding and meandering parameters." *Geol Soc Spec Publ* 75 (1993): 105-111.

14. Linard, Catherine, Nicolas Ponçon, Didier Fontenille, and Eric F Lambin. "A multi-agent simulation to assess the risk of malaria re-emergence in southern France." *Ecol Model* 220 (2009): 160-174.

15. Moriasi, Daniel N, Jeffrey G Arnold, Michael W. Van Liew, and Ronald L. Bingner, et al. "Model evaluation guidelines for systematic quantification of accuracy in watershed simulations." *Trans ASABE* 50 (2007): 885-900.

16. Nash, J Eamonn, and Jonh V Sutcliffe. "River flow forecasting through conceptual models part I A discussion of principles." *J Hydrol* 10 (1970): 282-290.

17. Santhi, Chinnasamy, Jeffrey G. Arnold, Jimmy R. Williams, and William A. Dugas, et al. "Validation of the swat model on a large rwer basin with point and nonpoint sources 1." *J Am Water Resour Assoc* 37 (2001): 1169-1188.

18. van Liew, MW, JG Arnold, and JD Garbrecht. "Hydrologic simulation on agricultural watersheds: Choosing between two models." *Trans ASAE* 46 (2003): 1539-1551.

19. Abbaspour, Karim C. "SWAT-CUP 2012: SWAT calibration and uncertainty programs a user manual." Eawag: Dübendorf, Switzerland 103 (2013).

How to cite this article: Tibebu, Yonatan, Hussen Ali, Fikru Fentan and Yohannes wodaje. "Integrated Hydrological and Hydraulic Models for Investigation of Channel Morphological Change and River Bank Erosion: A Case of Mersa River, Ethiopia." *Hydrol Current Res* 16 (2025): 567.